Predicting flotation behaviour – The interaction between froth stability and performance

S.J. Neethling and P.R. Brito-Parada

Department of Earth Science and Engineering, Imperial College London, London SW7 2AZ, UK

Abstract

Froth behaviour has a major impact on the overall performance of flotation cells, with the froth controlling the water recovery and entrainment, as well as having a significant impact on the recovery. Froth stability, including bubble coalescence and the bursting of the bubbles at the froth surface, are the key drivers of froth performance. Even though the froth stability is hard to directly control, it is important to understand how this stability impacts froth performance parameters such as the water recovery. In this paper it will be shown how a theoretical understanding of froth behaviour based on foam physics can be used to link stability to performance. The extent to which these simplified theoretical relationships can describe the complex behaviour seen in real flotation systems at both the laboratory and industrial scale are explored. The paper shows how bursting flux depends upon gas rate and how this influences the relationship between the gas rate and the water recovery.

Introduction

The performance of a flotation cells is the result of the complex interaction between phenomena in both the pulp and froth phases. The froth phase has a crucial role to play as it controls the amount of water recovered, and thus the amount of entrainment, as well as having a significant impact on the overall recovery. This is because the same coalescence and bursting of the bubbles that restricts the amount of water reporting to the concentrate, thus improving the grade, also allows particles to become detached from the bubbles, a portion of which will fall out of the froth and thus reduce the overall recovery of the cell via its impact on the froth recovery.

Understanding the link between froth stability and flotation performance is thus a key to being able to predict both the grade and recovery from these cells. In previous papers, models for various aspects of froth performance based on the fundamentals of foam physics have been introduced (Neethling et al., 2003a; Neethling, 2008; Neethling and Cilliers, 2008; Neethling and Cilliers, 2009). The theory behind these models will be briefly described at the beginning of this paper. These models, though, require information related to froth stability as inputs. In particular, they require the air recovery and surface bubble size as inputs, both of which are directly related to the stability of the particle laden films within the froth.

This paper will thus take a brief look at some of the theory related to the stability of these films, mainly to illustrate some of the complexity involved in the theoretical prediction of froth stability. While theory is enough to give clues as to the type of stability relationships to be expected, the relationship between mineralogy, particle size, reagent dosage and the stability of the films and, ultimately, the macroscopic stability of froth, is currently not well enough understood for theoretical predictions to be made.

This paper will thus take a semi-empirical approach in which the effect of air rate on the stability parameters is obtained from laboratory, pilot and industrial scale cells. These will then be combined with the theoretical froth performance models to predict how the changes in stability influence the trends in overall behaviour, with these predictions being compared to the actual experimental results.

The Physics of Froths

The theoretical predictions of the performance of flotation froths are based on the fact that they share much of the same physics as that of two-phase foams, the main difference being that the films in flotation froths are, to a large extent, particle stabilised rather than being directly surfactant stabilised.

Structurally these froths consist of bubbles separated by films, or lamellae, with these films meeting in threes at Plateau borders. As the interfaces of the Plateau borders curve sharply compared to any curvature of the films, capillarity will cause liquid to be sucked out of the films and into the Plateau borders until the films are thin enough that forces between the two film interfaces are able to counteract this suction. In two-phase systems this will be due to either electric double layer interactions or even direct steric interaction between the surfactant molecules, while in flotation froths the steric interaction between the particles loaded onto the films will provide much of the counteracting force. This suction of the liquid out of the films means that most of the liquid in a froth is to be found in the Plateau borders. These Plateau borders, in turn, meet at 4-fold vertices to form a network of interconnected channels. This means that, while the films are where most of the attached particles are located, the Plateau borders are where most of the liquid and unattached particles are to be found and are thus the focus of most of the modelling.

Liquid Drainage

In previous papers the modelling of liquid drainage in flotation froths has been described in detail (Neethling et al., 2000; Brito-Parada et al., 2012) and therefore only a brief description of the theory will be given in this paper. Within the Plateau border three forces need to be considered, namely gravity, capillarity and viscous dissipation. As Plateau border dimensions are small and flows are comparatively slow, inertial forces can be neglected and thus these forces can be balanced against one another in order to derive the foam drainage equation (Verbist et al., 1996) in which the liquid velocity vector, $\boldsymbol{v_l}$, is a function of the gas/bubble velocity vector, $\boldsymbol{v_g}$, and the cross-sectional Plateau border area, A:

$$\boldsymbol{v_l} = -\boldsymbol{k_1} A - \frac{k_2}{\sqrt{A}} \nabla A + \boldsymbol{v_g} \qquad (1.)$$

where $\boldsymbol{k_1} = \frac{\rho \boldsymbol{g}}{3 C_{PB} \mu}$ and $k_2 = \frac{\sqrt{\sqrt{3} - \frac{\pi}{2}}\gamma}{6 C_{PB} \mu}$

ρ, μ and γ are the density, viscosity and surface tension of the fluid, respectively, and $\boldsymbol{g}$ is the gravity acceleration vector. C_{PB} is a dimensionless Plateau border drag coefficient; it will have a value of approximately 50 if the fluid gas interfaces are immobile, but lower values as the interfacial mobility increases. This form of the drainage equation assumes that the viscous drag is dominated by losses in the Plateau borders rather than the vertices. This assumption is valid for foams in which there is low interfacial mobilities, which is likely to be the case in flotation froths as the interfaces are coated in particles.

The liquid content, ε, is related to the Plateau border area by the length of Plateau borders per volume of foam, λ, which is, in turn, a function of the bubble radius, R_b (using the equivalent spherical radius of the average bubble volume):

$$\varepsilon = \lambda A \qquad (2.)$$

where $\lambda = \frac{k_\lambda}{{R_b}^2}$

The pre-factor in this relationship, k_λ, is a function of the poly-dispersity of the bubbles, though for bubbles with a geometry of Kelvin cells it will be approximately 1.70 and for a random foam it will be (Kraynik et al., 2004):

$$k_\lambda = 2.047\frac{R_b}{R_{32}} + 0.024$$

where R_{32} is the Sauter mean radius of the bubbles, with the ratio between the Sauter mean and volume average radius being a measure of the poly-dispersity of the bubbles , with k_λ thus being approximately 2.071 for random mono-dispersed foams.

Liquid Recovery from a Flotation Froth

The foam drainage equation can be solved for the case of an overflowing foam. The key boundary condition is the top boundary, which is that the vertical liquid flux at the top surface must be zero. The gas flux through this surface will depend on the air recovery, α (fraction of air entering the cell that leaves as unburst bubbles), and the drainage rate of liquid relative to the foam at the top surface must thus equal this flux:

$$J_g(1-\alpha) = k_1 A_{top} + \frac{k_2}{\sqrt{A_{top}}}\frac{\partial A}{\partial y}\bigg|_{top} \qquad (3.)$$

where J_g is the gas flux into the froth and A_{top} the cross sectional area of the Plateau borders at the surface of the froth.

Figure 1 shows a typical simulation of the Plateau border area as a function of foam/froth depth. It can be seen that there is a change in the behaviour as the air recovery passes through 50%.

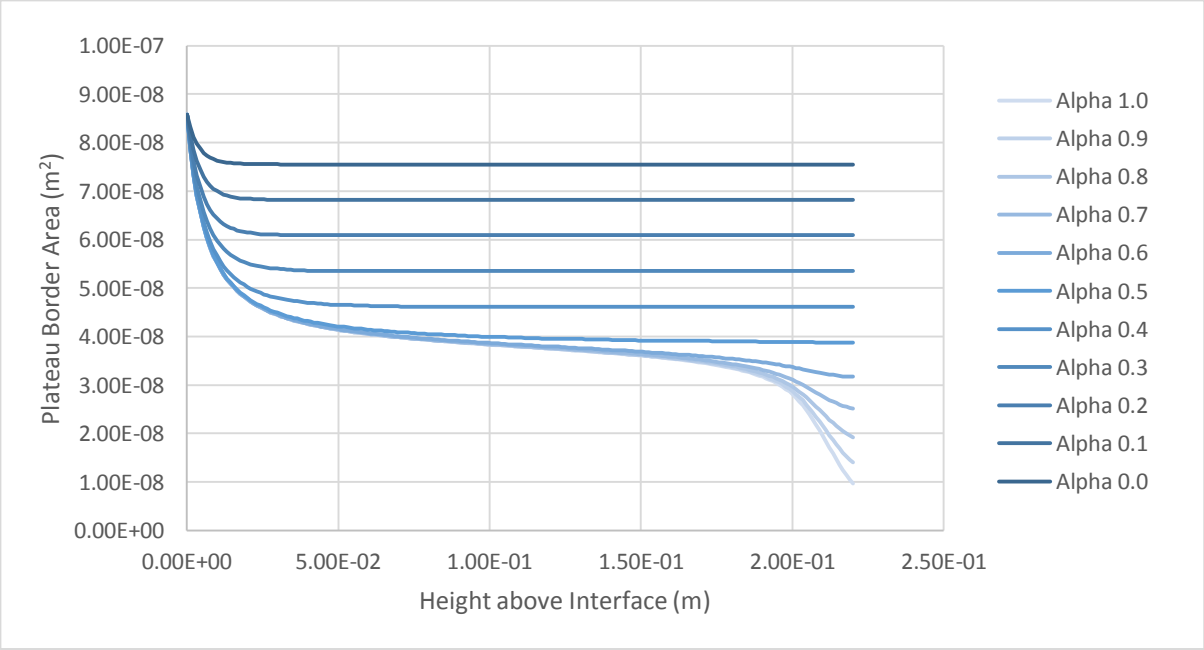


Figure 1: Plateau border area as a function of height in an overflowing foam for different air recoveries (based on Neethling et al. (2003a))

This is reflected in the equations for the amount of water recovered, which follows different relationships depending on whether the air recovery is above or below 50%. It has been demonstrated

in previous papers (Neethling et al., 2003a; Neethling, 2008; Neethling and Cilliers, 2009) that analytical approximations based on the foam drainage equation can be solved for the volumetric liquid flux, J_l:

$$J_l = \begin{cases} \frac{{J_g}^2 \lambda_{out}}{k_1}(1-\alpha)\alpha & if\ \alpha < 0.5 \\ \frac{{J_g}^2 \lambda_{out}}{4\,k_1} & if\ \alpha > 0.5 \end{cases} \qquad (4.)$$

where λ_{out} is the length of Plateau borders per volume based on an appropriately weighted overflowing bubble size. The approximation described in equation 4 holds for foams that are deeper than the capillary length scale, have viscous losses dominated by the Plateau borders and which have relatively low liquid contents in the overflowing foam (below about 5-10%), all of which hold for typical flotation froths. Most flotation froths, especially those in the rougher and scavenger banks, will have air recoveries below 50%.

In Neethling et al. (2003a,b) it was shown experimentally that equation 4 holds for a stable (air recovery of near 100%) foam, with the water flux showing a power law relationship to the gas flux, with an exponent very close to the theoretical value of 2 (see Figure 2).

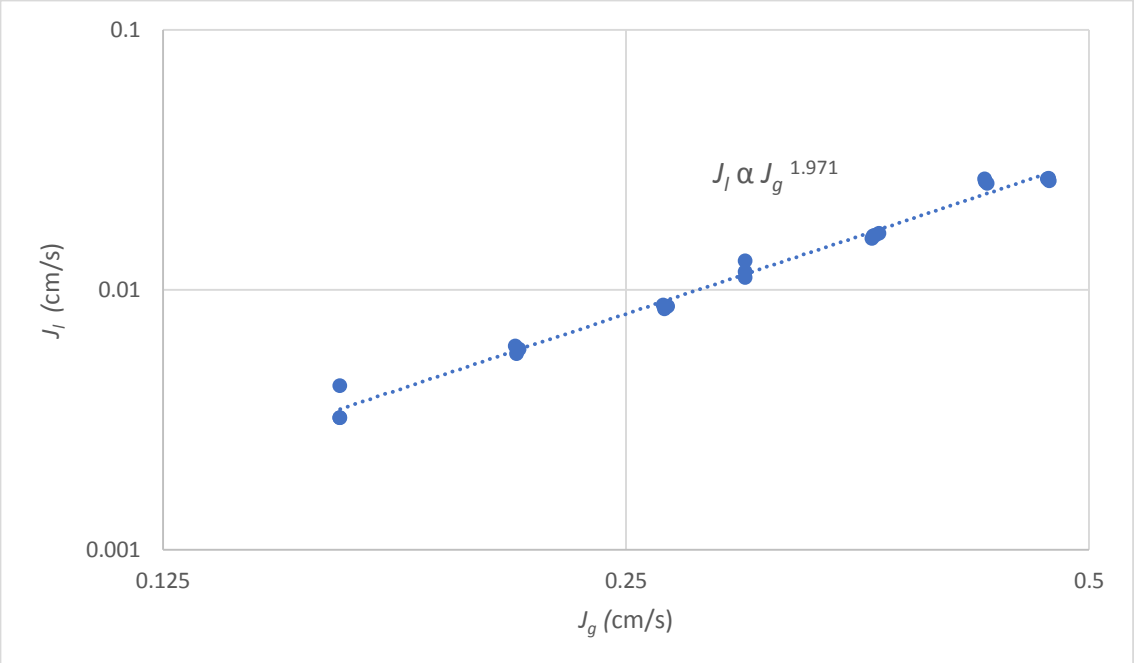


Figure 2: Liquid flux vs gas flux for a stable overflowing foam (based on data from Neethling et al. (2003b))

When looking at flotation data it does not, at first glance, appear to follow the same relationship when liquid flux is plotted against the gas flux, with the relationship being closer to linear with an offset on the gas rate axis (see Figure 2). The reason for the discrepancy is that the air recovery is also a function of the gas rate. One of the key objectives of this paper is thus to explore how the gas rate, air rate and liquid behaviour interact to produce the observed trends.

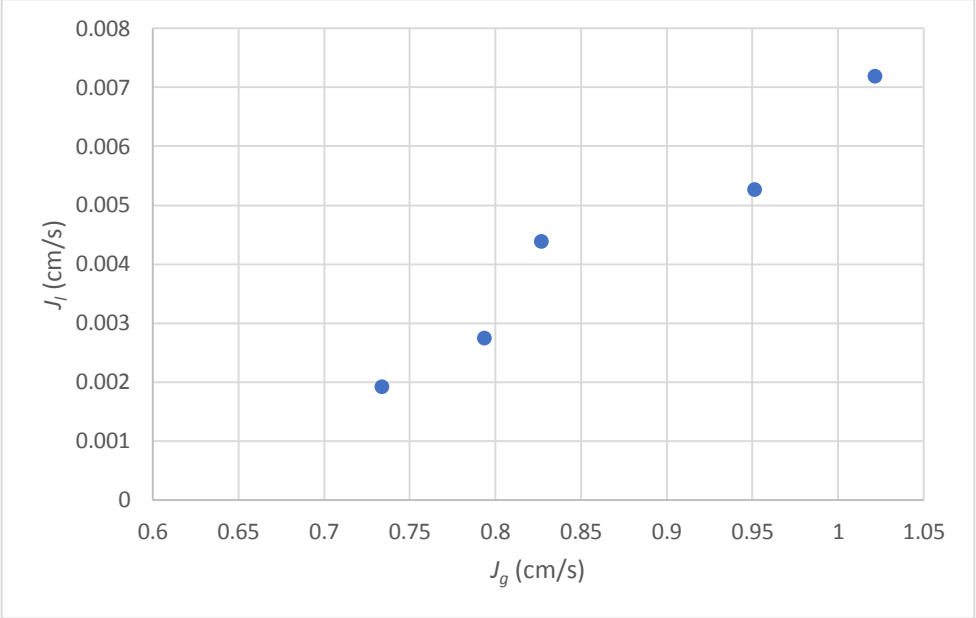


Figure 3: Liquid flux vs gas flux for a copper flotation rougher cell

Film Stability, Bursting and Air Recovery

The air recovery is, of course, intimately related to the rate at which bubbles burst at the surface of the froth, J_b:

$$J_b = J_g(1-\alpha) \qquad \text{or} \qquad \alpha = 1 - \frac{J_b}{J_g} \tag{5.}$$

Note that these equations assume that the cross-sectional area used to characterise the air flux, J_g, is the same as that of the bursting surface area. This will not be the case, for example, when the flotation cell design include crowders and launders.

The film stability of the bubbles at the surface is thus a crucial factor in the air recovery and thus also the water recovery. Flotation films typically have a critical pressure that needs to be exceeded before they can drain to failure. This critical pressure will depend on factors such as the particle loading on the interface and the contact angle and shape of the particles involved Morris et al., 2010, 2011). The pressure exerted on the film, $\Delta P_{Exerted}$, will be from a combination of the curvature of the Plateau border interface and surface tension:

$$\Delta P_{Exerted} = \frac{\gamma\sqrt{\sqrt{3}-\frac{\pi}{2}}}{\sqrt{A_{top}}} \tag{6.}$$

For froths with an air recovery less than 50% (which is typical of most flotation froths), the Plateau border area will be relatively constant with respect to height near the froth surface. By combining equations 5 and 3:

$$\text{if } \alpha < 0.5 \qquad J_b \approx k_1 A_{top} \tag{7.}$$

This implies that at lower air recoveries the pressure exerted on the film is directly related to the bursting rate:

$$\text{if } \alpha < 0.5 \qquad J_b \approx \frac{k_1 \gamma^2 \left(\sqrt{3} - \frac{\pi}{2}\right)}{\Delta P_{Exerted}{}^2} \tag{8.}$$

Since the films in a flotation froth are comparatively thick (they are stabilised by particles and thus must be of the order of the particle size thick) compared to the very thin films encountered in 2 phase systems (these films typically need to have thinned to 10s of nanometres thick before electric double layer interactions are strong enough to stabilise them), they drain quickly and therefore the average pressure exerted on them at the bursting surface of the froth is likely to be close to the critical pressure required for failure.

Since this critical pressure depends on loading, it is complex to predict as loading will vary not only with the attachment in the pulp phase, but also with the extent of coalescence that has occurred over the depth of the froth. This is because coalescence results in only a portion of the particles attached to the failing film becoming detached Neethling, 2008) and thus the loading on the remaining films increases (the surface area of the bubbles decreases more rapidly than the mass of particles attached to them).

As the prediction or even direct measurement of the critical pressure required for failure is very complex, it is thus desirable to approach this problem from the other side; if we can measure the bursting rate of the bubbles we can infer their stability behaviour and thus obtain insights into how this stability varies with operating parameters such as the air rate.

Measuring Bubble Bursting Rates

Attempts have been made to directly measure the bursting flux by measuring the size and frequency of film failures at the surface (Morar et al, 2012). While useful for understanding where bubbles are bursting and which size bubbles are bursting, it is not reliable for the accurate quantitative measurement of the bursting flux. For the experimental bursting rates presented in this paper, a more indirect measure is used, based on the same methodology as used to measure the air recovery from the cell Hadler and Cilliers, 2009; Norori-McCormac et al., 2017). This measure is based on the fact that any air that is lost through the bursting surface is the difference between the air entering the cell and that overflowing as unburst bubbles:

$$J_b = J_g - \frac{v_{overflow} l_{lip} h_{over}}{A_{Cell}} \tag{9.}$$

where $v_{overflow}$ is the velocity of the froth over the lip of the cell and which is measured using image analysis based on video taken by a camera mounted vertically above the edge of the cell; h_{over} is the height of the froth above the lip and is measured using laser based distance measurements; and l_{lip} is the length of the lip of the cell. When multiplied together these give the volumetric flowrate of gas into the concentrate (assuming that the liquid content is low enough to have little impact on the volumetric rate, which is usually a reasonable assumption for most rougher and scavenger cells). A_{Cell} is the cross-sectional area of the cell and appears in the equation as it is what is used to convert the gas rate and bursting rate into a flux.

The main source of uncertainty in this method for measuring the bursting rate is usually in the measurement of the gas rate into the cell. This is not an issue in laboratory and pilot scale cells, where accurate rotameter based gas rate measurements are available, but in industrial measurements it can be an issue as the online air rate measurements are often not very well calibrated. The alternative on plant is to directly measure air fluxes, but this is not only time consuming, as the flux will vary spatially, requiring multiple measurements for a good average to be obtained, but is also often not feasible due to the a lack of suitable access at the top of the cells for the flux measurement columns to be inserted.

This is less of an issue in the measurement of air recovery trends, where a constant percentage error in the measured air rate would preserve the trend but cause errors in the quantitative values, but is potentially a serious issue in the measurement of the bursting rate as this involves calculating the difference between two values and thus an error in one will not only influence the values obtained, but also the trends observed. For this reason, the trends in the bursting rate will first be investigated at the laboratory and pilot scale, where there is confidence in the values measured, before investigating them in industrial cells.

Experimental Bursting Rates

In Figure 4 the bursting flux is shown as a function of the air flux into the cell for a continuous laboratory scale flotation cell. It shows that the bursting rate is relatively constant, but with a slight increase with increasing gas rate. Similar trends are observed for industrial flotation cells, with Figure 5 showing the bursting flux versus gas flux in for the first cell in the rougher bank of a number of different concentrators.

The discussion in the previous section shows that the bursting flux is directly related to the inherent stability of the films. This implies that for both the laboratory and industrial froths the inherent film stability decreases with increasing gas rate, doing so in a well behaved, monotonic fashion (albeit with a degree of scatter, especially in some of the industrial measurements). The main reason for this decrease is likely to be that the loading on the bubbles will decrease with increasing air rate. The total amount of material floated will increase with increasing gas rate, but will do so at a slower rate than the flux of surface area, thus resulting in a decrease in the loading per surface area, which, together with the composition and size of the particles, is the important consideration in froth flotation.

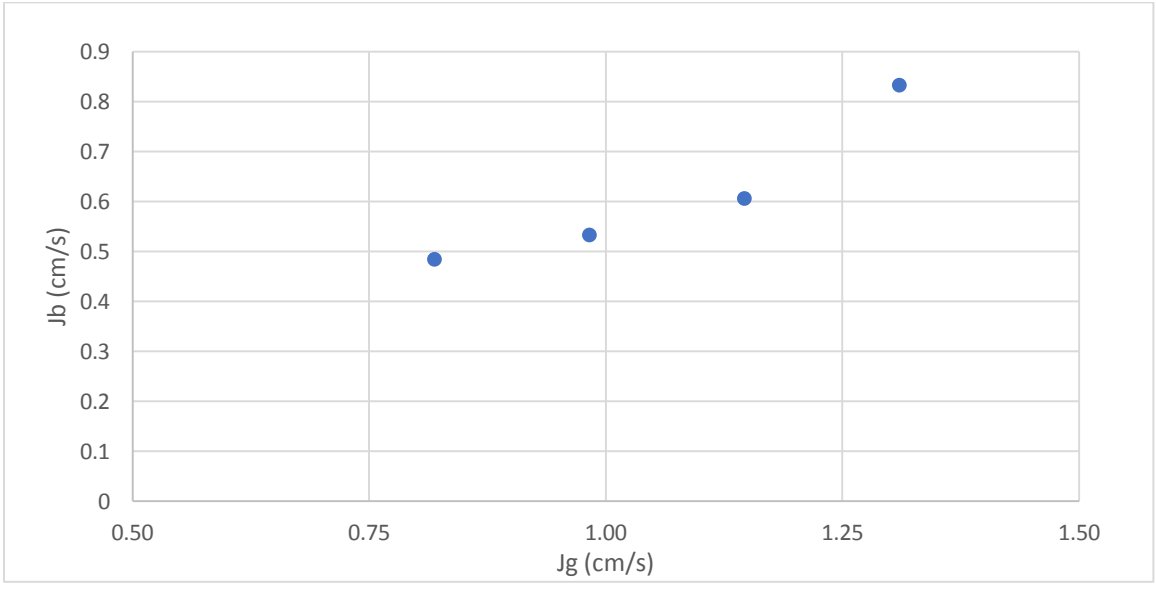


Figure 4: Bursting rate vs gas flux for a bench scale cell reverse flotation of magnetite from silica for a conventional pulp zone design

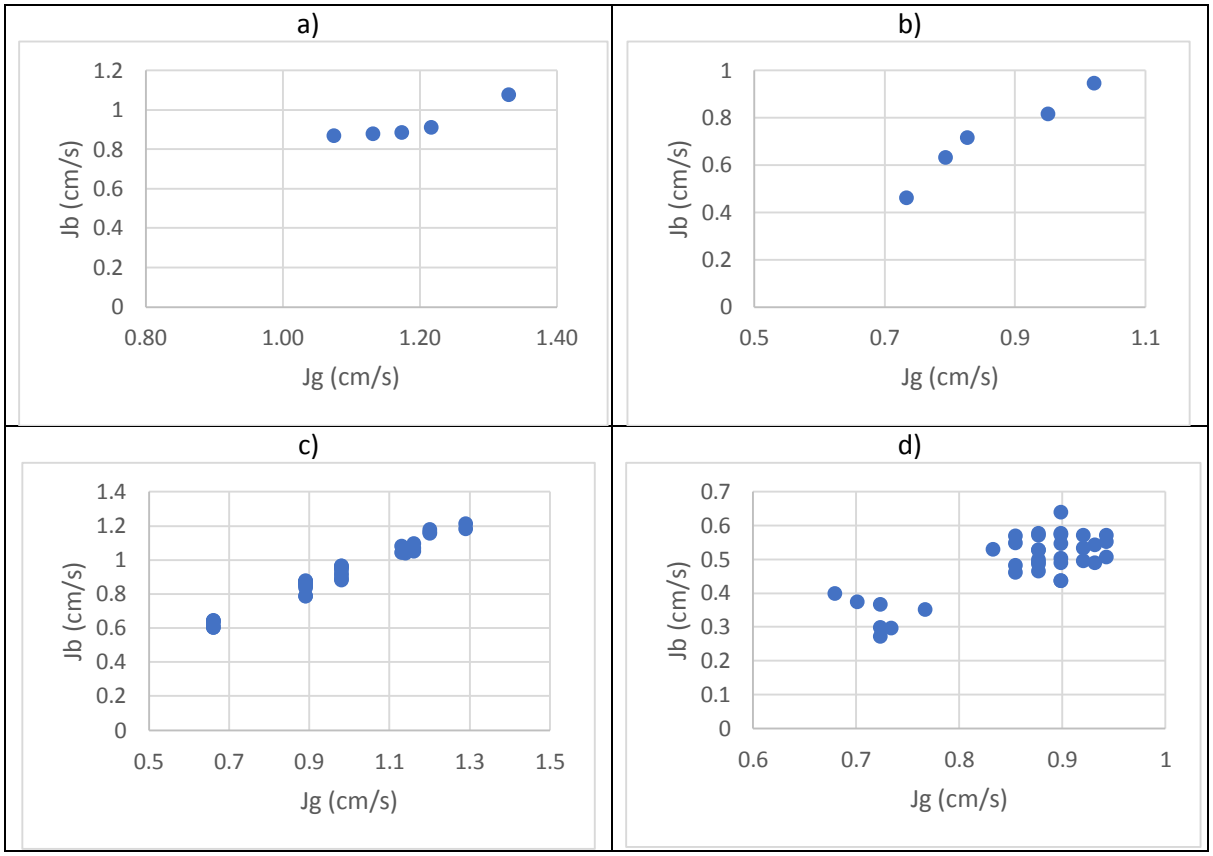


Figure 5: Bursting rate vs gas flux for industrial rougher cells. a) and b) first rougher cell in two platinum concentrators. c) and d) first rougher cell in two copper concentrators

The Implications of Bursting Rate Trends for Water Recovery

The relationship between water recovery, gas rate and bursting rate can be predicted by combining equations 4 and 5:

$$if\ \alpha < 0.5 \qquad J_l = \frac{\lambda_{out}}{k_1}\left(J_g - J_b\right)J_b \qquad (10.)$$

(note that if $\alpha > 0.5$ $\quad J_l = \frac{\lambda_{out}}{4k_1}{J_g}^2$ irrespective of the bursting rate or its relationship to J_g)

A constant bursting rate would imply that the air recovery would asymptote towards one as the gas rate into the cell is increased (see equation 5). This is not what is seen in either laboratory or industrial scale measurements of air recovery, which tends to go through a maximum as the gas rate into the cell is increased (Hadler and Cilliers, 2009; Norori-McCormac et al., 2017). Making this assumption does, though, imply a trend in the water recovery that is closer to that which is experimentally observed when compared to the squared relationship that is predicted when there is either no bursting or no dependency of the bursting rate on the air rate. By examining equation 10, it can be seen that, if the overflowing bubble size (and thus λ_{out}) remains constant with increasing air rate, a constant bursting rate implies that the water recovery increases linearly with gas rate, with an offset on the gas rate axis equal to the bursting rate. This linear increase will continue until the air recovery hits 50%, above which there will be a quadratic increase in the liquid recovery, with no dependency on the bursting rate.

Most of the trends in bursting rate, at least to a first order approximation, show a background bursting rate, J_{b0}, with a subsequent linear increase in bursting rate with the gas rate:

$$J_b \approx J_{b0} + a\,J_g \tag{11.}$$

This still does not imply an air recovery that goes through a maximum. Instead it would result in an air recovery that asymptotes towards a value of $1 - a$ as J_g increases. The value of a must be less than one as a value above one would imply a bursting rate that is higher than the gas rate for all gas rates. The value will also typically be above zero as the inherent stability of the froth will virtually always decrease with increasing air rate as the amount of stabilising particles and surfactant available per film area will decrease and the disturbances introduced into the froth will typically increase.

If the bursting rate increases linearly with gas rate according to equation 11, then the water recovery follows the following relationship:

$$if\ \alpha < 0.5 \qquad J_l = \frac{\lambda_{out}}{k_1}\left((1-2a)J_{b0}\,J_g - {J_{b0}}^2 + (1-a)a\,{J_g}^2\right) \tag{12.}$$

There is thus once again an intercept on the gas rate axis that is associated with the bursting rate being equal to the gas rate ($J_b = J_g = J_{b0}/(1-a)$), but above this value, and in the absence of any change in the overflowing bubble size with gas rate, there is a more rapid than linear increase in the water recovery.

Even though the linear increase in bursting is close to what is observed experimentally, the implied trend in the air recovery is not. In virtually all the flotation systems that we have studied, at both laboratory and industrial scale, air recovery goes through a maximum rather than asymptoting towards a constant value. This implies that, even though they are quite subtle in terms of the bursting rate trends, higher order dependencies are important in the bursting rate relationship. The simplest model that captures the experimentally observed maximum in the air recovery is a second order relationship between gas rate and bursting:

$$J_b \approx J_{b0} + a\,J_g + b\,{J_g}^2 \tag{13.}$$

The pre-factor for the second order term can either be expressed in terms of a characteristic flux, J_{char}, or, potentially more usefully, as a function of the gas flux at which the maximum in the air recovery is observed, $J_{g\,max}$:

$$b = \frac{1}{J_{char}} = \frac{J_{b0}}{{J_{g\,max}}^2} \tag{14.}$$

Even though substituting equation 13 into equation 10 introduces a large number of additional higher order terms (out to 4th order in J_g), the net result is actually a water recovery that increases closer to linearly than that with a linear increase with gas rate.

In Figure 6Figure 6 all the bursting rates from a range of different laboratory experiments are plotted against gas rate. Despite some of these experiments being run with different pulp zone designs, there is still quite a well-defined trend between the experimental bursting flux and the gas flux into the cell. It can also be seen that both the linear and 2nd order trends provide plausible fits to the data.

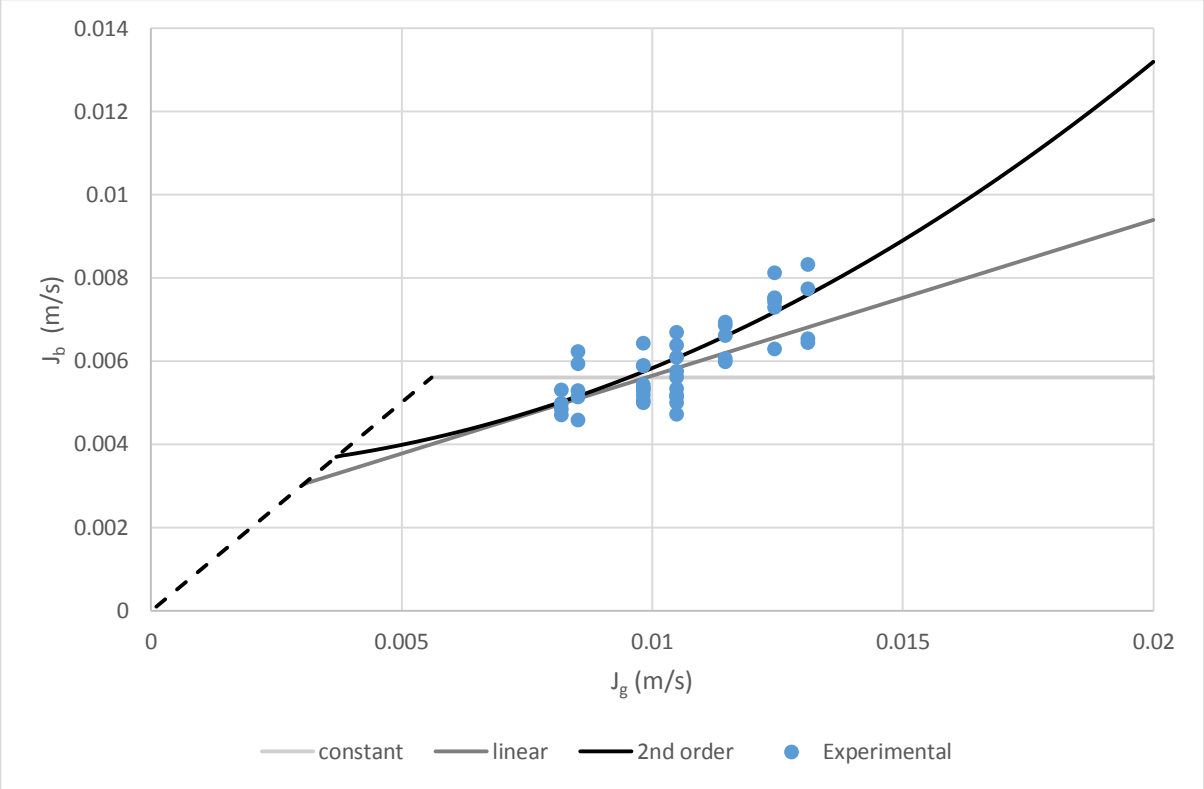


Figure 6: Bursting rate against gas rate. Experimental data compared to constant, linear and 2nd order with gas flux bursting models. In the constant model $J_b = 0.0056\ m/s$. In the linear model $J_{b0} = 0.0019\ m/s$ and $a = 0.375$. In the 2nd order model $J_{b0} = 0.003369\ m/s$, $a = 0.0012$ and $J_{g\,max} = 0.0117\ m/s$.Note that in addition to the data from figure 4, this graph also includes data from experiments with different pulp zone inserts.

The air recoveries can also be calculated based on the bursting rates and as these are simply a different way of presenting the same data, both the linear and 2nd order models again provide plausible fits to the data (see Figure 7).

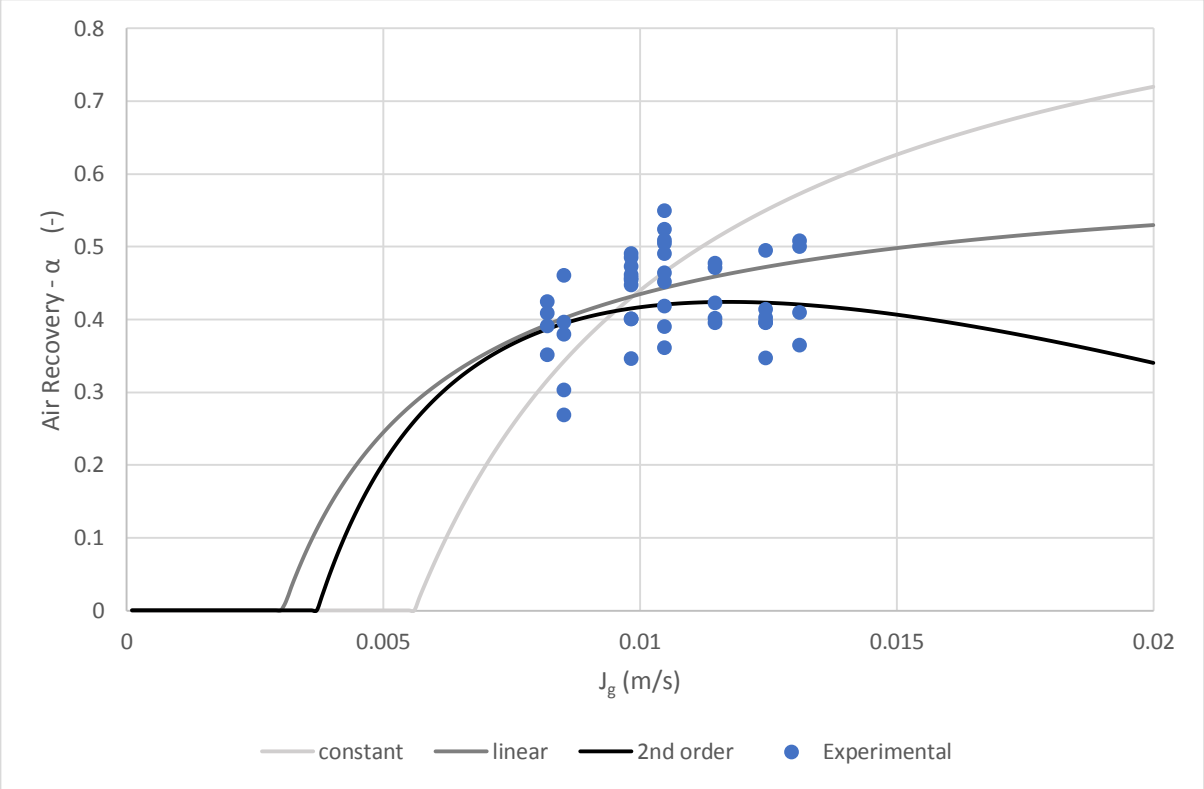


Figure 7: Experimental air recovery versus gas flux and comparisons to air recovery trends calculated based on a constant, linear and 2nd order with gas flux bursting models.

Unlike the calculation of the air recovery based on the bursting rate, the calculation of the water recovery is actually a prediction as it assumes that the form of the model is correct. As the laboratory experiments presented above were not intended for the study of the effect of froth stability on water recovery, the water flux was not recorded for all the experiments. For all those experiments for which it was recorded, the results are plotted against the trends predicted from the models based on different bursting behaviours (see Figure 8).

In order to make the predictions of the water recovery based on equation 10, the value for λ_{out}/k_1 is required. k_1 can be estimated based on the density and rheology of typical concentrate slurries, which leaves the overflowing bubble size required to calculate λ_{out} as the only independent fitting parameter. While it is known that this bubble size will be a function of the gas rate as well, in order to produce these model predictions, it is assumed to be constant. The best fit between experimental and model based liquid flux vs gas flux relationships is obtained at a very reasonable value for the average overflowing bubble size of 0.57 cm.

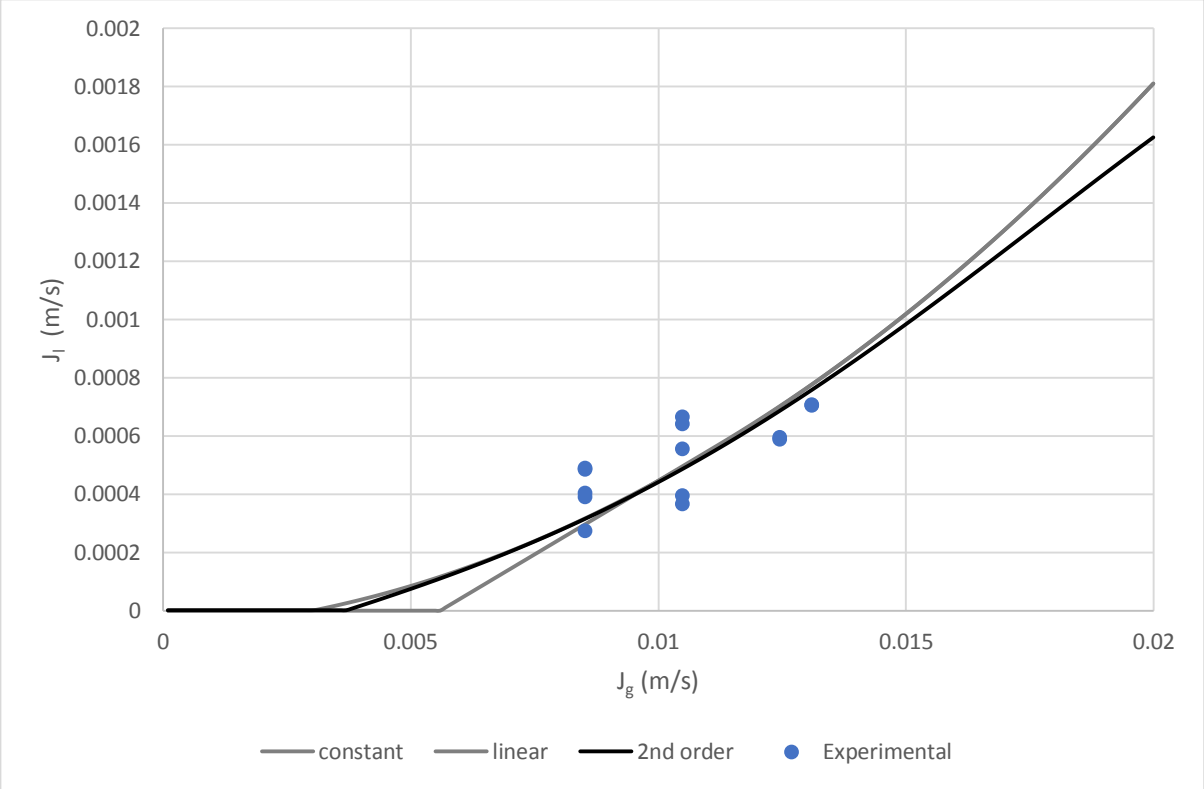


Figure 8: Experimental water recoveries vs gas flux and a comparison against predictions for the water flux based on different bursting models. Note that in the model based predictions the surface bubble size is assumed to be constant with respect to gas rate, with this bubble size being used as the only fitting parameter. A realistic average overflowing bubble radius of 0.57 cm was found to provide the best fit between the model and experimental results.

Conclusions

This paper has demonstrated how the bursting rate of bubbles in a flotation froth depends upon the gas rate and the impact that this has on the recovery of liquid from the cell. In particular, it demonstrates why there is typically a near linear increase in the water recovery with gas rate, with an intercept on the gas rate axis.

This paper has not addressed the influence of the overflowing bubble size on the water recovery, which is the other important stability related impact. While the theoretical models can account for this impact, actually predicting the overflowing bubble size is hard, with the relationship to air rate, froth depth and other operating parameters being far more system dependent than the bursting behaviour.

References

Brito-Parada, P.R., Neethling, S.J., Cilliers, J.J., 2012. The advantages of using mesh adaptivity when modelling the drainage of liquid in froths. Minerals Engineering 33, 80-86.

Hadler, K., Cilliers, J.J., 2009. The relationship between the peak in air recovery and flotation bank performance. Minerals Engineering 22 451-455.

Kraynik, A.M., Reinelt, D.A., van Swol, F., 2004. Structure of random foam. Physical Review Letters 93 (20), 208301-1-208301-4.

Morar, S.H., Bradshaw, D.J., Harris, M.C., 2012. The use of the froth surface lamellae burst rate as a flotation froth stability measurement. Minerals Engineering 36-38, 152-159.

Morris, G., Neethling, S.J., Cilliers, J.J., 2010. The effects of hydrophobicity and orientation of cubic particles on the stability of thin films. Minerals Engineering 23, 979-984.

Morris, G., Neethling, S.J., Cilliers, J.J., 2011. An investigation of the stable orientations of orthorhombic particles in a thin film and their effect on its critical failure pressure. Journal of Colloid and Interface Science 361, 370-380

Neethling, S.J., 2008. Simple approximations for estimating froth recovery. International Journal of Mineral Processing 89, 44-52.

Neethling, S.J., Cilliers, J.J., 2008. Predicting air recovery in flotation cells. Minerals Engineering 21, 937-943.

Neethling, S.J., Cilliers, J.J., 2009. The entrainment factor in flotation: Model for particle size and other operating parameter effects. International Journal of Mineral Processing 93, 141-148.

Neethling, S.J., Cilliers, J.J., Woodburn, E.T., 2000. Prediction of the water distribution in flowing foams. Chemical Engineering Science 55, 4021-4028.

Neethling, S.J., Lee, H.T., Cilliers, J.J., 2003a. Simple relationships for predicting the recovery of liquid from flowing foams and froths. Minerals Engineering 16, 1123-1130.

Neethling, S.J., Lee, H.T., Cilliers, J.J., 2003b. The recovery of liquid from flowing foams. J. Phys.: Cond. Mat. 15, 1563–1576

Norori-McCormac, A., Brito-Parada, P.R., Hadler, K., Cole, K., Cilliers, J.J., 2017. The effect of particle size distribution on froth stability in flotation. Separation and Purification Technology 184, 240-247.

Verbist, G., Weaire, D., Kraynik, A.M., 1996. The foam drainage equation. Journal of Physics: Condensed Matter 8 (21), 3715-3731.